Optical Free-Form Couplers for High-density Integrated Photonics (OFFCHIP): A Universal Optical Interface

Citation: Yu, Shaoliang et al. "Optical Free-Form Couplers for High-density Integrated Photonics (OFFCHIP): A Universal Optical Interface." Journal of Lightwave Technology 38, 13 (January 2020): 3358 - 3365 © 2020 IEEE

As Published: http://dx.doi.org/10.1109/jlt.2020.2971724

Publisher: Institute of Electrical and Electronics Engineers (IEEE)

Persistent URL: https://hdl.handle.net/1721.1/128033

Version: Author's final manuscript: final author's manuscript post peer review, without publisher's formatting or copy editing

Optical Free-Form Couplers for High-density Integrated Photonics (OFFCHIP): a universal optical interface

Shaoliang Yu, Haijie Zuo, Xiaochen Sun, *Member*, *IEEE*, Jifeng Liu, *Senior Member*, *IEEE*, Tian Gu, *Member*, *IEEE*, and Juejun Hu, *Member*, *IEEE*

(Invited Paper)

***Abstract*—Coupling of light between different photonic devices, for example on-chip waveguides, fibers, and free-space optical elements, is an essential function enabling integrated optical systems. Efficient optical coupling demands matching the optical mode profiles and effective indices in two devices, and often changing propagation direction of the light. To date, such coupling is pre-dominantly accomplished via direct butt coupling of two devices, or meticulously optimized diffraction gratings. In this paper, we present a new coupling scheme based on microfabricated free-form optical reflectors. The free-form reflector simultaneously achieves the functions of light beam re-direction and shaping (for mode matching), and can be versatilely adapted for coupling between photonic chips, fibers, and free-space surface-incident devices. We show that this technology uniquely fulfills all key performance requirements for optical interfaces with exceptionally low coupling loss (0.2 – 0.3 dB per coupler), large bandwidth (over half an octave), high density (large 2-D coupler arrays), polarization diversity, and superior alignment tolerance commensurate with passive alignment techniques. Preliminary experimental validation demonstrates waveguide-to-fiber coupling with a low insertion loss (IL) of 0.9 dB. We foresee that the technology will become a promising solution to the chip-level photonic interconnection and packaging challenges plaguing integrated photonics.**

***Index Terms*—integrated photonics, coupling, free-form optics, waveguides, fibers, free-space optics, packaging.**

I. Introduction

OPTICALLY interfacing different photonic devices and propagation media is a basic function necessary for construction of complex integrated optical systems. Some common examples of such optical interface include waveguide-to-fiber coupling, chip-to-chip or chip-to-interposer coupling, and waveguide-to-free-space coupling. In general, the optical interface performs two functions: shaping the optical mode(s) to maximize overlap integral between modes of the two devices; and re-directing the light to match the propagation direction in the devices, if necessary. The optical interfacing approach chosen usually plays a critical role in defining the boundaries of performance and costs for scalable photonic interconnections and packaging.

Traditionally, an optical interface assumes one of two common configurations: butt coupling or grating coupling [1]–[14]. In the former case, optical output facets of the two devices (e.g. two waveguides or a waveguide and a fiber) are placed in close proximity and aligned to each other. Mode transformers (often of adiabatic types) are usually fabricated on the end facets of one or both of the devices to mitigate mode mismatch and improve the coupling efficiency [15], [16]. A lower index material can be further deposited on top of a tapered Si waveguide to form an adiabatic mode transformer between the high-index-contrast (HIC) and low-index-contrast (LIC) waveguides, expanding the optical mode in both horizontal and vertical directions [17]–[23]. In multi-layer structures, high-index and low-index layers are stacked on each other with tapered structures to allow transformation of the optical mode [24]–[27]. In addition to inverse tapers, subwavelength grating structures have also been engraved into the waveguides to convert the spot size for edge coupling [28]–[31]. So far broadband low-loss waveguide-to-fiber butt coupling has been demonstrated with ILs down to ~ 0.4 dB [32], [33]. One the other hand, the butt coupling scheme suffers from several limitations. First, the affordable density by this scheme is limited by the lateral pitch of the devices. In the case of fiber-to-chip coupling, a semi-standard fiber array pitch of 125 μm stipulates a limited density of 8 connections per millimeter chip perimeter inadequate for meeting the I/O bandwidth target of electronic chips [34]. Second, butt coupling typically places stringent requirements on optical alignment due to the small mode size in HIC waveguide devices, necessitating precise but time-consuming active alignment during the optical assembly

This work was supported by ARPA-E under the ENLITENED Program (Award Number: DE-AR0000847).

Shaoliang Yu, Haijie Zuo, Juejun Hu, and Tian Gu are with the Department of Materials Science & Engineering and Materials Research Laboratory, Massachusetts Institute of Technology, Cambridge, MA 02139 USA (e-mails: yusl@mit.edu; gutian@mit.edu).

Jifeng Liu is with Thayer School of Engineering, Dartmouth College, 14 Engineering Drive, Hanover, NH 03755 USA.

Xiaochen Sun is with LaXense Inc., 1730 W Cameron Ave., Suite 100, West Covina, CA 91790 USA.

process. Last but not least, butt coupling is only applicable to chip-level characterization after the photonic chips have been diced from a full wafer but is generally not suitable for wafer-scale testing and screening.

In contrast, grating coupling, another popular candidate for optical interfacing, offers 2-D connectivity and the expediency of high-throughput wafer-level device testing [12], [35]–[50]. Near-unity coupling efficiency has been theoretically predicted [51], [52] and an impressive IL as low as 0.36 dB has been experimentally demonstrated [53], albeit both at a single wavelength. Another advantage of grating coupling is that it is readily scalable to high channel density using 2-D coupler arrays and potentially relaxed mechanical alignment tolerance [54]. However, the main drawback of grating coupling is its limited spectral bandwidth. For waveguide-to-fiber coupling, gratings typically exhibit a 1-dB bandwidth of 30-50 nm near the telecom wavelength, which precludes their application in wavelength division multiplexing (WDM) communication networks. Similarly, most low-loss grating couplers also exhibit strong polarization dependence [55]. Additionally, to attain high coupling efficiency, grating coupler designs often involve nonorthodox structures such as embedded mirrors and multilayer overlay which may not necessarily be compatible with standard silicon photonic foundry processing [46], [51]–[53], [56]–[60]. Multi-level etched and slanted grating couplers also predict high coupling efficiency while posing additional challenges for the fabrication process [3], [61]–[65].

In sum, existing butt and grating coupling schemes do not fulfill all the essential requirements for an optical interface and thus pose performance and cost trade-offs with limited scalability. Butt coupling is limited in terms of bandwidth density and accessibility to chip edge facets, whereas narrow spectral bandwidth is the main challenge with grating couplers. In this paper, we propose and experimentally demonstrate a new optical interface (OFFCHIP) uniquely featuring low coupling loss, exceptionally broad bandwidth, polarization diversity, high and scalable bandwidth density, and tailorable, large alignment tolerance ideal for chip-scale dense optical interconnects, and high-throughput photonic packaging and assembly. The coupling concept, design rationale and application examples are discussed in the following sections.

II. Optical Free-Form Couplers for High-density Integrated Photonics (OFFCHIP): the Concept

The proposed optical coupling interface, OFFCHIP, is based on a free-form optical reflector attached to and index-matched to the end facet of a LIC waveguide. An adiabatic mode transformer can be used to further transition the optical mode from the LIC waveguide to a HIC waveguide with vanishingly low losses. The use of a LIC waveguide is critical as it not only diminishes index mismatch (e.g. between a fiber and an on-chip waveguide) and Fresnel reflection, but also reduces angle-dependent aberration of the free-form optics. The reflector geometry is optimized to carry out two functions simultaneously: 1) re-direct the light beam propagation path (usually by 90° but arbitrary deflection angles are possible) via total internal reflection; and 2) re-shape the beam such that it matches the mode in the output device, thereby enabling very high coupling efficiency.

A particularly simple form of the reflector design assumes a quadratic surface geometry. The output mode of a LIC waveguide can be well approximated with a point source of a small numerical aperture (NA) or divergence angle. An ellipsoidal reflector surface can therefore act as a waveguide-to-waveguide coupler re-focusing the output light from a LIC waveguide into another, provided that both waveguide point sources are placed at the focal points of the ellipsoidal surface. In the same vein, a parabolic reflector can collimate the output light from a LIC waveguide positioned at the focus, and the collimated beam diameter can be readily adjusted by changing the distance of the waveguide output to the reflector surface. Since standard single-mode optical fibers has a small numerical aperture, the fiber mode can be well matched to a collimated beam with a similar diameter. A parabolic reflector therefore efficiently couples light from an on-chip waveguide to a fiber. In addition to its remarkable simplicity (and high performance as shown later), the quadratic surface design also provides an excellent starting point (aka heuristic) for advanced designs derived from topology optimization algorithms [66].

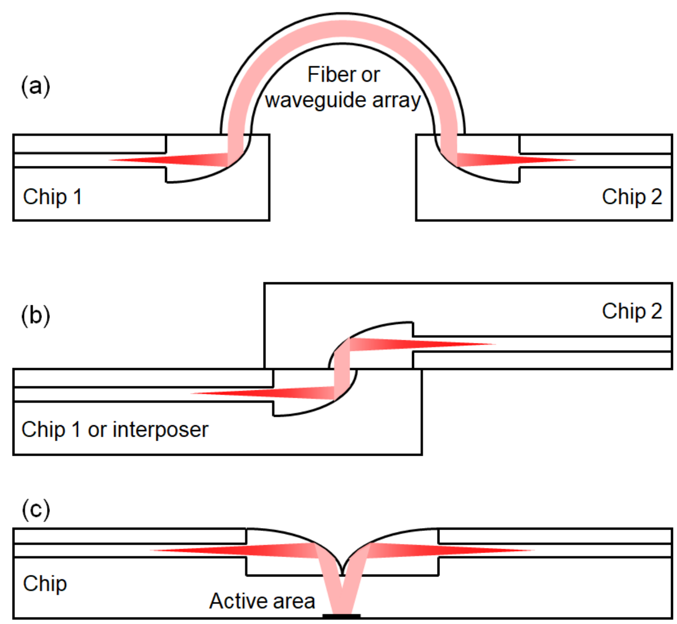

Fig. 1. Several embodiments of the OFFCHIP optical interfaces for (a) waveguide-to-fiber coupling; (b) waveguide-to-waveguide (chip-to-chip or chip-to-interposer) coupling; and (c) waveguide coupling to surface-incident devices.

The OFFCHIP platform is universally applicable to a wide array of optical coupling scenarios as schematically illustrated in Fig. 1. The parabolic reflectors can be used as optical I/Os for photonic chips connecting with optical fiber or polymer waveguide ribbon arrays (Fig. 1a). Alternatively, they can function as waveguide-to-waveguide couplers by mating two identical parabolic reflectors (Fig. 1b). Another embodiment of the OFFCHIP platform involves using the reflector to collimate a waveguide output, which then is directed towards and reflected by a surface-incident device before re-coupled to a second waveguide by a second parabolic reflector (Fig. 1c). This coupling scheme offers an efficient optical interface between in-plane optical waveguides and surface-incident devices such as single-mode vertical-cavity surface-emitting lasers (VCSELs), multi-quantum well (MQW) modulators, and free-space photodetectors to introduce various optoelectronic functionalities. Moreover, the OFFCHIP platform can also facilitate coupling of light from on-chip waveguides to the free space with user-defined beam shapes for applications such as optical trapping and sorting, sensing, laser writing, and free-space optical communications.

The OFFCHIP platform uniquely combines minimal coupling loss, broadband and polarization-diverse operation, high bandwidth density, and large alignment tolerance. The large design degrees of freedom accessible with the 3-D free-form surface enables precise mode conversion to bridge mode size and shape mismatches between two coupling devices, a prerequisite for high optical efficiency. The use of a reflective element underlies the design's extreme broadband performance, as reflective optics are immune to dispersion effects which inherently limit the bandwidth of diffractive or refractive optical components. Unlike butt coupling which demands an exposed chip facet to accommodate the coupling fiber or another chip, the reflector can be fabricated inside an etched trench where a waveguide terminates. The free-form reflectors can therefore be fabricated to form large 2-D arrays, allowing high-density optical I/O not bound by the perimeter length of photonic chips. The reflective couplers are also compatible with array alignment, which is crucial to scalable, high-throughput photonic packaging and assembly. Finally, since the reflector acts as a mode size expander, the design offers improved alignment tolerance compared to direct butt coupling.

III. Coupler Designs

In this section, we describe the design of several embodiments of the OFFCHIP optical interface.

A. *Waveguide-to-fiber coupler*

Coupling from on-chip waveguides to optical fibers is considered a major technical bottleneck in scalable photonic chip packaging due to the large mode size and effective index mismatch between optical fibers and HIC waveguides. Our OFFCHIP platform provides a promising solution to the chip I/O challenge, where light from on-chip HIC waveguide is first adiabatically transformed into a LIC waveguide and then directed to an optical fiber. As discussed above, the free-form reflector in this case assumes a parabolic shape to convert the diverging output from a LIC waveguide to a collimated beam whose diameter matches that of a single-mode fiber. A specific design example is presented in Fig. 2. In the simulation, the waveguide has a core size of 2.3 μm × 2.3 μm and core and cladding indices n_{core} = 1.543 and n_{clad} = 1.525, respectively. The parameters match those of our fabricated devices (Section IV) and ensure single-mode operation of the waveguide at 850 nm wavelength. A Nufern 780-HP fiber with a mode field diameter of 5 μm and a flat cleaved facet is chosen as it offers broadband single-mode operation around the target wavelength.

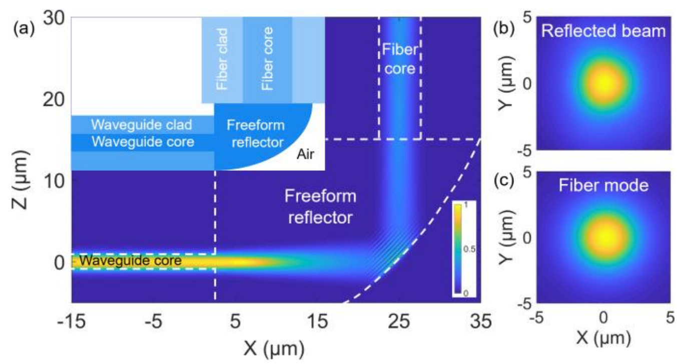

Fig. 2. (a) The OFFCHIP waveguide-to-fiber coupler simulated using 3-D finite-difference time-domain (FDTD) showing the optical intensity distribution across the center plane; inset schematically shows the device layout; (b, c) intensity profiles of (b) the beam exiting from the reflective coupler; and (c) the mode of a Nufern 780-HP single-mode fiber.

It is further assumed that the fiber is bonded to the reflective coupler using an index-matched epoxy (n = 1.543) to eliminate Fresnel reflection losses. The position and size of the parabolic reflector are optimized to maximize the overlap integral between the profile of beam exiting from the coupler and the optical fiber mode, thereby minimizing IL (Figs. 2b & 2c). The optimized coupler occupies a small on-chip footprint of 30 μm (X) × 10 μm (Y) and is thus amenable to high-density 2-D fiber array integration.

Figure 3a plots the simulated ILs of the waveguide-to-fiber coupler. The simulation shows that the coupler offers low ILs of < 0.3 dB across an exceptionally broad spectral band of 700 – 1050 nm (half an octave) for both transverse electric (TE) and transverse magnetic (TM) polarizations. A minimal IL of 0.18 dB is achieved for the TE polarization at 770 nm wavelength, corresponding to a peak coupling efficiency of 96%. This remarkable broadband performance benefits from the non-dispersive nature of reflective optical elements. The coupler also exhibits good tolerance to misalignment as shown in Fig. 3b. In the out-of-plane (Z) direction, the reflected beam is almost collimated, which accounts for the large tolerance (over 25 μm) to fiber offset along the Z-direction. In the in-plane (X and Y) directions, the alignment tolerance is determined by the fiber mode field diameter and can be further increased by incorporating mode expanders if desired [67]. The coupler features a 1-dB alignment tolerance of ± 1.1 μm at 850 nm wavelength. Optimized coupler designs at the long-wave 1550 nm telecom band claim a 1-dB alignment tolerance of ± 2.3 μm [68]. This large alignment tolerance facilitates surface-normal, high-throughput passive alignment of optical fiber arrays to on-chip waveguides, possibly aided by mechanical alignment features. The results highlight the key advantages of the OFFCHIP waveguide-to-fiber coupler: low IL, ultra-broadband and polarization-diverse operation, high integration density, compatibility with wafer-level testing, and large alignment tolerance. The coupling scheme also places minimum requirement on the coupling fibers' facet preparation. These features are essential features for a scalable, high-throughput, high-performance, and low-cost photonic chip packaging

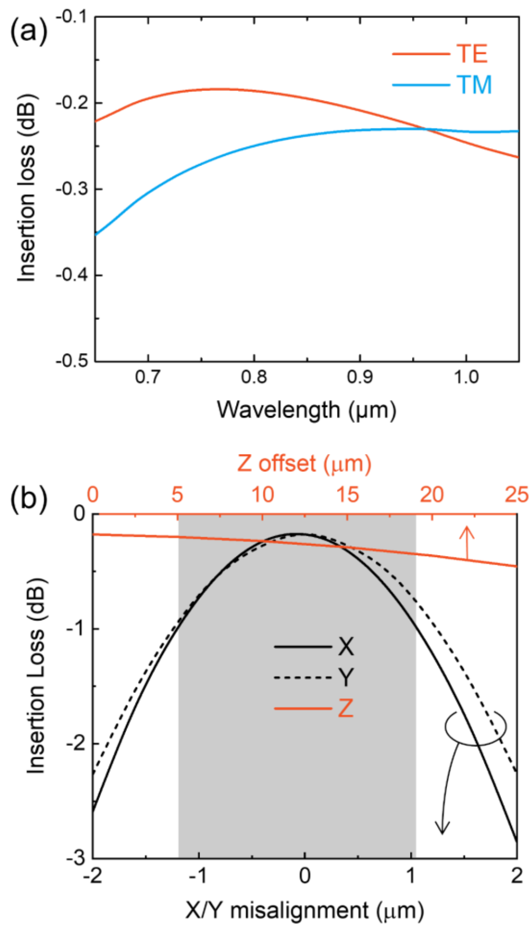

Fig. 3. (a) Wavelength and polarization dependent ILs of the optimized waveguide-to-fiber coupler simulated using 3-D FDTD; (b) tolerance of the coupler IL to misalignment in X, Y, and Z directions. The gray box corresponds to 1-dB alignment tolerance in the in-plane (X and Y) directions.

solution.

B. Waveguide-to-waveguide (chip-to-chip or chip-to-interposer) coupler

Direct coupling of light from an optical waveguide on a chip to a second waveguide on another chip is a useful function for interfacing photonic chips with optical interposers or flexible waveguide ribbons, communications between different chips in a multi-chip module (MCM), or coupling of light from chips to optical printed circuit boards (PCBs) [69]–[74]. Such inter-chip coupling was traditionally implemented with 45° mirrors [75]–[78] or grating couplers [14]. However, the former approach furnishes limited coupling efficiency due to the inevitable wave front distortion induced by the flat 45° mirrors, whereas gratings are inherently wavelength sensitive.

The OFFCHIP platform offers a high-efficiency, broadband solution for inter-chip coupling. Figure 4 depicts a specific embodiment of the inter-chip coupler. Here the waveguides assume an identical configuration (core size and core/cladding indices) to that in Fig. 2. Similar to the waveguide-to-fiber coupler, the optimized waveguide-to-waveguide coupler claims broadband, low-loss performance with an IL consistently below 0.5 dB between 650 – 950 nm wavelengths for both TE and TM polarizations, and an IL as low as 0.22 dB for TE polarization at 760 nm wavelength. Tolerance to misalignment of the coupler is investigated through numerical FDTD simulations and the results are summarized in Fig. 4c. The in-plane (X and Y) 1-dB alignment tolerance is ± 1.3 μm. Unlike the case of waveguide-to-fiber coupler where the tolerance is bound by the fiber mode field diameter, here the inter-chip alignment tolerance can be improved simply by increasing the coupler size to further expand the reflected beam diameter. Moreover, the very large alignment tolerance in the out-of-plane (Z) direction (> 35 μm) indicates that efficacy of the coupling scheme is minimally affected by unfavorable surface conditions of the chips (e.g. surface unevenness) and the presence of dust particles, both of which are often culprits limiting the yield of photonic packaging processes. The high performance and excellent assembly tolerance qualify the OFFCHIP coupling scheme as an appealing solution for inter-chip optical interfacing.

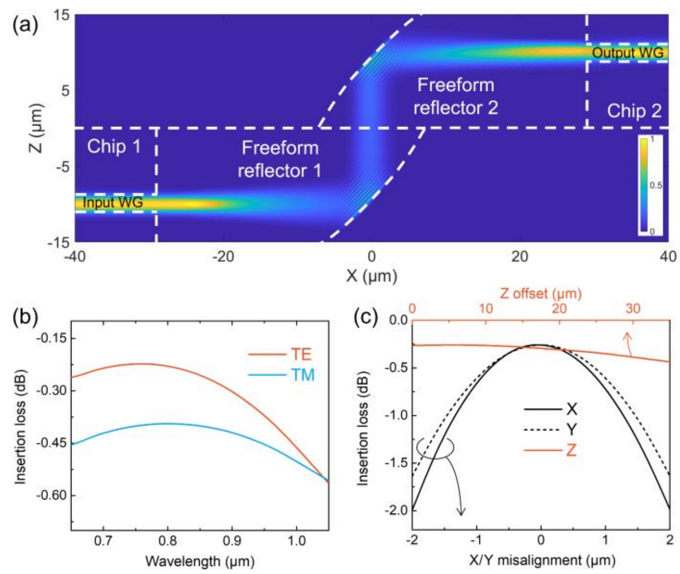

Fig. 4. (a) The waveguide-to-waveguide coupler modeled using 3-D FDTD showing the optical intensity distribution across the waveguide (WG) center plane; (b) simulated wavelength and polarization dependent ILs of the optimized waveguide-to-waveguide coupler; (b) tolerance of the coupler IL to misalignment in X, Y, and Z directions.

C. Waveguide integration of surface-incident devices

Many optoelectronic devices employ a surface-incident configuration to facilitate coupling with light incident from or emitted to free space. The examples of such devices include VCSELs, MQW modulators, and free-space photodetectors. Their surface-incident configuration, nevertheless, makes their coupling with waveguides and integration with planar photonic integrated circuits (PICs) challenging. In the multi-mode regime, flat and curved mirrors, prism couplers, and facet couplers have been implemented to couple light from/to these surface-incident devices [79]–[83]. Integration of these devices with single-mode waveguides, while currently lacking a mature solution, potentially brings major benefits to PICs: for instance, high-efficiency single-mode VCSELs and surface-plasmon-enhanced MQW modulators can significantly enhance the energy efficiency of optical interconnects when desirable optical coupling and integration conditions are met [84].

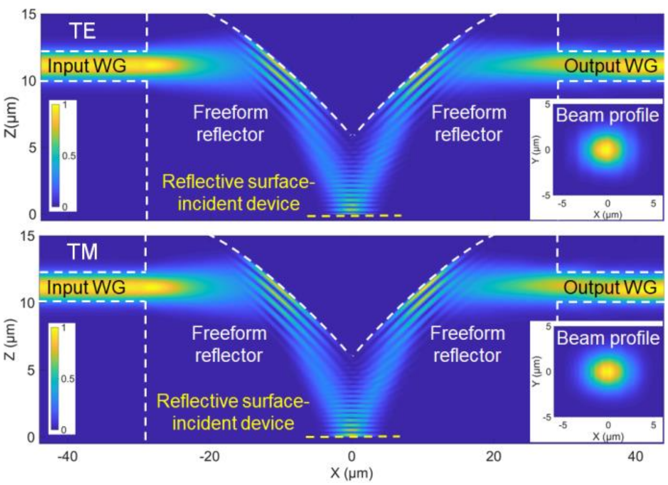

Fig. 5. Single-mode waveguide integration with a surface-incident device in a reflective configuration: the optical intensity distribution across the device center plane simulated using 3-D FDTD is plotted for (top) TE and (bottom) TM polarized inputs from the waveguide. Insets display the intensity distribution of the beam impinging on the surface-incident device.

Figure 5 illustrates FDTD simulation results of single-mode waveguide coupling with surface-incident devices via the free-form reflectors depicted in Fig. 1c. A pair of parabolic reflectors are used to collimate the output from a single-mode waveguide with a 40° incident angle with respect to the device, and re-focus the beam reflected from the surface-incident device (e.g. an MQW modulator) back to the waveguide. In the simulation, the waveguides assume the same configuration (core size and core/cladding indices) as that in Fig. 2. The simulation reveals high coupling efficiencies of 94% (0.27 dB IL) and 95% (0.22 dB IL) at 850 nm wavelength for TE and TM polarized inputs, respectively. Insets in Fig. 5 plot the optical intensity profiles at the surface-incident device's top surface. The small mode field diameter (8.5 μm, $1/e^2$ of the maximum intensity) of the optical beam further implies that the integration scheme can apply to surface-incident devices with a small active area and minimal RC time constant for high-speed operation. The freeform reflective surfaces can be further optimized to tailor the beam properties (e.g., angle of incidence, divergences, intensity distribution, etc.) incident on the surface-normal device for desirable optoelectronic responses. The OFFCHIP platform therefore provides a facile route for integration of traditional free-space devices with single-mode waveguide PICs.

IV. Experimental Demonstration of a Low-Loss Free-Form Waveguide-to-Fiber Coupler

We prototyped the free-form waveguide-to-fiber coupler using two photon polymerization (TPP). TPP has already been validated to be a powerful tool for on-demand fabrication of 3-D optical structures with critical dimensions well below the classical diffraction limit. Recent advances in parallel TPP printing further promise dramatic improvements in fabrication throughput using this technology [85], [86]. Some examples of photonic structures fabricated using TPP include 3-D photonic crystals [87]–[90], photonic wire bonds [91]–[93], multi-lens objectives [94], [95], free-form refractive optical couplers [96], [97], and fiber to waveguide connector[98]. Compared to previously demonstrated refractive optical couplers, our design achieves significantly enhanced optical efficiencies and ultra-broadband performance through concurrent suppression of both chromatic aberration and monochromatic angle-dependent aberrations with simple quadratic reflective surfaces.

In our process, polymer waveguides were first fabricated following our previously established protocols [99]. A trench with a depth of 15 μm was then etched into the polymer layers to define the waveguide facet to which the reflectors are attached. The free-form reflectors were then sculpted using TPP in the photosensitive polymer OrmoComp (Micro Resist Technology GmbH) using the Photonic Professional GT 3-D printer station (Nanoscribe GmbH). The process decouples 3-D fabrication of the free-form couplers with patterning of planar waveguide circuits such that the latter can be performed using standard lithographic methods with high throughput. Our optimized process also achieves high alignment accuracy between the pre-patterned waveguides and the subsequently added coupler structures (Fig. 6a) with average misalignment of 0.16 μm (X-direction), 0.13 μm (Y-direction), and 0.2 μm (Z-direction). The high precision is adequate to guarantee negligible loss due to coupler-waveguide misalignment. The fabricated 3-D couplers also feature a low root-mean-square (RMS) surface roughness of (8 ± 1) nm, implying negligible optical losses due to roughness scattering.

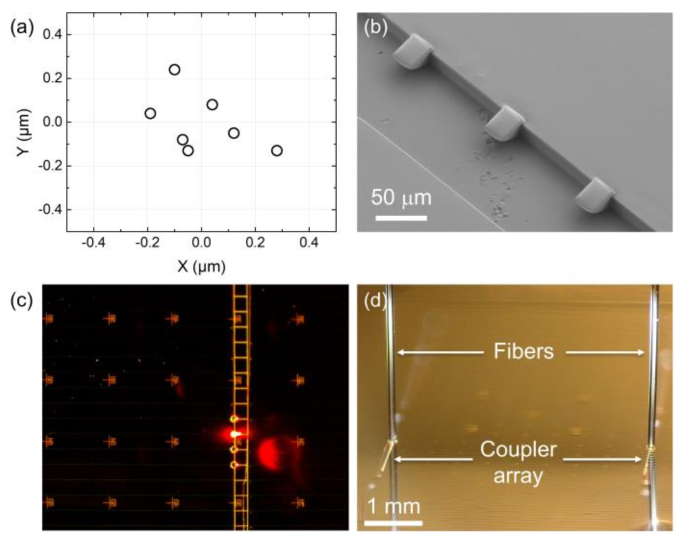

Fig. 6. (a) Measured relative misalignment distributions between the waveguides and TPP-fabricated couplers; (b) tilted-view SEM image of fabricated coupler arrays; (c) top-view optical micrograph of light output exiting from the waveguide and entering free space through the reflective coupler; (d) a photo of fibers coupling to an on-chip waveguide via the reflective couplers.

To characterize the reflective optical couplers, broadband light from a superluminescent diode (QSDM-860-8B, QPhotonics LLC, center wavelength 856 nm, spectral full width at half maximum 45 nm) was coupled into a Nufern 780-HP single-mode fiber with flat cleaved facets. A pair of fiber probes were aligned to two couplers connecting to both ends of the waveguides, and the transmitted power was measured using a photodetector (818-IS-1, Newport Corporation). The coupler IL was calculated by comparing the optical power output from a single fiber versus the transmitted power through the fiber-waveguide-fiber assembly. Our measurement revealed an IL of (0.9 ± 0.2) dB averaged over five fabricated couplers. The measured IL is higher than the simulated value of 0.2 dB due to deviations of the reflector shape from the designed geometry caused by volume shrinkage of the polymer during the photo-induced cross-linking process. Despite the largely unoptimized process, the experimentally demonstrated IL of 0.9 dB is still on par with the performances of state-of-the-art edge or grating couplers.

Further process optimization is underway to improve the shape fidelity and performance of the coupler.

V. Conclusions

In this paper, we propose and experimentally validate a free-form reflective optical coupler design applicable to interfacing a wide range of photonic devices including waveguides, fibers, surface-incident optoelectronic devices, and free-space components. Compared to conventional optical coupling schemes, the proposed OFFCHIP platform uniquely combines superior coupling efficiency, ultra-broadband and polarization-diverse operation, high integration density, and large, tailorable alignment tolerance commensurate with passive alignment. The technology therefore offers a high-performance and scalable solution for photonic packaging and assembly.

References

[1] G. Roelkens, D. Van Thourhout, and R. Baets, “High efficiency Silicon-on-Insulator grating coupler based on a poly-Silicon overlay,” *Opt. Express*, vol. 14, no. 24, p. 11622, 2006.

[2] D. Vermeulen *et al.*, “High-efficiency fiber-to-chip grating couplers realized using an advanced CMOS-compatible Silicon-On-Insulator platform,” *Opt. Express*, vol. 18, no. 17, p. 18278, Aug. 2010.

[3] D. Benedikovic *et al.*, “High-directionality fiber-chip grating coupler with interleaved trenches and subwavelength index-matching structure,” *Opt. Lett.*, vol. 40, no. 18, p. 4190, Sep. 2015.

[4] C. Alonso-Ramos, A. Ortega-Moñux, I. Molina-Fernández, P. Cheben, L. Zavargo-Peche, and R. Halir, “Efficient fiber-to-chip grating coupler for micrometric SOI rib waveguides,” *Opt. Express*, vol. 18, no. 14, p. 15189, Jul. 2010.

[5] L. Carroll *et al.*, “Photonic Packaging: Transforming Silicon Photonic Integrated Circuits into Photonic Devices,” *Appl. Sci.*, vol. 6, no. 12, p. 426, Dec. 2016.

[6] R. Marchetti, C. Lacava, L. Carroll, K. Gradkowski, and P. Minzioni, “Coupling strategies for silicon photonics integrated chips [Invited],” *Photonics Res.*, vol. 7, no. 2, p. 201, 2019.

[7] G. Roelkens *et al.*, “High efficiency diffractive grating couplers for interfacing a single mode optical fiber with a nanophotonic silicon-on-insulator waveguide circuit,” *Appl. Phys. Lett.*, vol. 92, no. 13, 2008.

[8] M. L. Dakss, L. Kuhn, P. F. Heidrich, and B. A. Scott, “Grating coupler for efficient excitation of optical guided waves in thin films,” *Appl. Phys. Lett.*, vol. 16, no. 12, pp. 523–525, 1970.

[9] D. Taillaert *et al.*, “An out-of-plane grating coupler for efficient butt-coupling between compact planar waveguides and single-mode fibers,” *IEEE J. Quantum Electron.*, vol. 38, no. 7, pp. 949–955, Jul. 2002.

[10] D. Taillaert, P. Bienstman, and R. Baets, “Compact efficient broadband grating coupler for silicon-on-insulator waveguides,” *Opt. Lett.*, vol. 29, no. 23, p. 2749, Dec. 2004.

[11] R. Orobtchouk, A. Layadi, H. Gualous, D. Pascal, A. Koster, and S. Laval, “High-efficiency light coupling in a submicrometric silicon-on-insulator waveguide,” *Appl. Opt.*, vol. 39, no. 31, p. 5773, Nov. 2000.

[12] X. Chen, C. Li, C. K. Y. Fung, S. M. G. Lo, and H. K. Tsang, “Apodized Waveguide Grating Couplers for Efficient Coupling to Optical Fibers,” *IEEE Photonics Technol. Lett.*, vol. 22, no. 15, pp. 1156–1158, Aug. 2010.

[13] R. Halir, P. Cheben, S. Janz, D.-X. Xu, Í. Molina-Fernández, and J. G. Wangüemert-Pérez, “Waveguide grating coupler with subwavelength microstructures,” *Opt. Lett.*, vol. 34, no. 9, p. 1408, May 2009.

[14] G. Li *et al.*, “Ultralow-loss, high-density SOI optical waveguide routing for macrochip interconnects,” *Opt. Express*, vol. 20, no. 11, p. 12035, May 2012.

[15] V. R. Almeida, R. R. Panepucci, and M. Lipson, “Nanotaper for compact mode conversion,” *Opt. Lett.*, vol. 28, no. 15, p. 1302, Aug. 2003.

[16] L. Vivien, S. Laval, E. Cassan, X. Le Roux, and D. Pascal, “2-D Taper for Low-Loss Coupling between Polarization-Insensitive Microwaveguides and Single-Mode Optical Fibers,” *J. Light. Technol.*, vol. 21, no. 10, pp. 2429–2433, 2003.

[17] T. Shoji, T. Tsuchizawa, T. Watanabe, K. Yamada, and H. Morita, “Low loss mode size converter from 0.3 µm square Si wire waveguides to singlemode fibres,” *Electron. Lett.*, vol. 38, no. 25, pp. 1669–1670, Dec. 2002.

[18] G. Roelkens, P. Dumon, W. Bogaerts, D. van Thourhout, and R. Baets, “Efficient silicon-on-insulator fiber coupler fabricated using 248-nm-deep UV lithography,” *IEEE Photonics Technol. Lett.*, vol. 17, no. 12, pp. 2613–2615, Dec. 2005.

[19] S. McNab, N. Moll, and Y. Vlasov, “Ultra-low loss photonic integrated circuit with membrane-type photonic crystal waveguides,” *Opt. Express*, vol. 11, no. 22, p. 2927, Nov. 2003.

[20] R. Dangel *et al.*, “Polymer Waveguides Enabling Scalable Low-Loss Adiabatic Optical Coupling for Silicon Photonics,” *IEEE J. Sel. Top. Quantum Electron.*, vol. 24, no. 4, pp. 1–11, Jul. 2018.

[21] T. Tsuchizawa *et al.*, “Microphotonics devices based on silicon microfabrication technology,” *IEEE J. Sel. Top. Quantum Electron.*, vol. 11, no. 1, pp. 232–239, Jan. 2005.

[22] B. Ben Bakir *et al.*, “Low-Loss ($<$ 1 dB) and Polarization-Insensitive Edge Fiber Couplers Fabricated on 200-mm Silicon-on-Insulator Wafers,” *IEEE Photonics Technol. Lett.*, vol. 22, no. 11, pp. 739–741, Jun. 2010.

[23] J. U. N. Auriyal, “Fiber-to-chip fusion splicing for low-loss photonic packaging,” *Optica*, vol. 6, no. 5, pp. 3–6, 2019.

[24] Q. Fang *et al.*, “Suspended optical fiber-to-waveguide mode size converter for Silicon photonics,” *Opt. Express*, vol. 18, no. 8, p. 7763, Apr. 2010.

[25] J. V. Galán, P. Sanchis, G. Sánchez, and J. Martí, “Polarization insensitive low-loss coupling technique between SOI waveguides and high mode field diameter single-mode fibers,” *Opt. Express*, vol. 15, no. 11, p. 7058, May 2007.

[26] D. Dai, S. He, and H. K. Tsang, “Bilevel mode converter between a silicon nanowire waveguide and a larger waveguide,” *J. Light. Technol.*, vol. 24, no. 6, pp. 2428–2433, Jun. 2006.

[27] Z. Pan *et al.*, “Quasi-vertical tapers for polymer-waveguide-based interboard optical interconnects,” *Photonics Res.*, vol. 3, no. 6, p. 317, Dec. 2015.

[28] P. Cheben *et al.*, “Broadband polarization independent nanophotonic coupler for silicon waveguides with ultra-high efficiency,” *Opt. Express*, vol. 23, no. 17, p. 22553, Aug. 2015.

[29] M. Papes *et al.*, “Fiber-chip edge coupler with large mode size for silicon photonic wire waveguides,” *Opt. Express*, vol. 24, no. 5, p. 5026, Mar. 2016.

[30] P. Cheben *et al.*, “Refractive index engineering with subwavelength gratings for efficient microphotonic couplers and planar waveguide multiplexers,” *Opt. Lett.*, vol. 35, no. 15, p. 2526, Aug. 2010.

[31] P. Cheben, D.-X. Xu, S. Janz, and A. Densmore, “Subwavelength waveguide grating for mode conversion and light coupling in integrated optics,” *Opt. Express*, vol. 14, no. 11, p. 4695, 2006.

[32] M. Pu, L. Liu, H. Ou, K. Yvind, and J. M. Hvam, “Ultra-low-loss inverted taper coupler for silicon-on-insulator ridge waveguide,” *Opt. Commun.*, vol. 283, no. 19, pp. 3678–3682, Oct. 2010.

[33] R. Sun *et al.*, “High performance asymmetric graded index coupler with integrated lens for high index waveguides,” *Appl. Phys. Lett.*, vol. 90, no. 20, 2007.

[34] D. A. B. Miller, “Device requirements for optical interconnects to silicon chips,” *Proc. IEEE*, vol. 97, no. 7, pp. 1166–1185, Jul. 2009.

[35] D. Pascal, R. Orobtchouk, A. Layadi, A. Koster, and S. Laval, “Optimized coupling of a Gaussian beam into an optical waveguide with a grating coupler: comparison of experimental and theoretical results,” *Appl. Opt.*, vol. 36, no. 12, p. 2443, Apr. 1997.

[36] L. He *et al.*, “A high-efficiency nonuniform grating coupler realized with 248-nm optical lithography,” *IEEE Photonics Technol. Lett.*, vol. 25, no. 14, pp. 1358–1361, 2013.

[37] R. Marchetti *et al.*, “High-efficiency grating-couplers: Demonstration of a new design strategy,” *Sci. Rep.*, vol. 7, no. 1, Dec. 2017.

[38] A. Bozzola, L. Carroll, D. Gerace, I. Cristiani, and L. C. Andreani, “Optimising apodized grating couplers in a pure SOI platform to −05 dB coupling efficiency,” *Opt. Express*, vol. 23, no. 12, p. 16289, Jun. 2015.

[39] X. Chen and H. K. Tsang, “Nanoholes grating couplers for coupling between silicon-on-insulator waveguides and optical fibers,” *IEEE Photonics J.*, vol. 1, no. 3, pp. 184–190, Sep. 2009.

[40] X. Chen, K. Xu, Z. Cheng, C. K. Y. Fung, and H. K. Tsang, “Wideband subwavelength gratings for coupling between silicon-on-insulator waveguides and optical fibers,” *Opt. Lett.*, vol. 37, no. 17, p. 3483, Sep. 2012.

[41] R. Halir *et al.*, “Continuously apodized fiber-to-chip surface grating coupler with refractive index engineered subwavelength structure,” *Opt. Lett.*, vol. 35, no. 19, p. 3243, Oct. 2010.

[42] D. Benedikovic *et al.*, “Subwavelength index engineered surface grating coupler with sub-decibel efficiency for 220-nm silicon-on-insulator waveguides,” *Opt. Express*, vol. 23, no. 17, p. 22628, Aug. 2015.

[43] F. Van Laere *et al.*, “Compact Focusing Grating Couplers for Silicon-on-Insulator Integrated Circuits,” *IEEE Photonics Technol. Lett.*, vol. 19, no. 23, pp. 1919–1921, Dec. 2007.

[44] G. Roelkens, D. Vermeulen, S. Selvaraja, R. Halir, W. Bogaerts, and D. Van Thourhout, “Grating-based optical fiber interfaces for silicon-on-insulator photonic integrated circuits,” *IEEE J. Sel. Top. Quantum Electron.*, vol. 17, no. 3, pp. 571–580, May 2011.

[45] C. Li, K. S. Chee, J. Tao, H. Zhang, M. Yu, and G. Q. Lo, “Silicon photonics packaging with lateral fiber coupling to apodized grating coupler embedded circuit,” *Opt. Express*, vol. 22, no. 20, p. 24235, Oct. 2014.

[46] W. S. Zaoui *et al.*, “Bridging the gap between optical fibers and silicon photonic integrated circuits,” *Opt. Express*, vol. 22, no. 2, p. 1277, 2014.

[47] B. Snyder and P. O’Brien, “Packaging process for grating-coupled silicon photonic waveguides using angle-polished fibers,” *IEEE Trans. Components, Packag. Manuf. Technol.*, vol. 3, no. 6, pp. 954–959, 2013.

[48] N. Pavarelli *et al.*, “Optical and electronic packaging processes for silicon photonic systems,” *J. Light. Technol.*, vol. 33, no. 5, pp. 991–997, Mar. 2015.

[49] T. W. Ang, G. T. Reed, A. Vonsovici, A. G. R. Evans, P. R. Routley, and M. R. Josey, “Highly efficient unibond silicon-on-insulator blazed grating couplers,” *Appl. Phys. Lett.*, vol. 77, no. 25, pp. 4214–4216, Dec. 2000.

[50] M. K. Emsley, O. Dosunmu, and M. S. Ünlü, “Silicon substrates with buried distributed Bragg reflectors for resonant cavity-enhanced optoelectronics,” *IEEE J. Sel. Top. Quantum Electron.*, vol. 8, no. 4, pp. 948–955, Jul. 2002.

[51] L. Zhu, W. Yang, and C. Chang-Hasnain, “Very high efficiency optical coupler for silicon nanophotonic waveguide and single mode optical fiber,” *Opt. Express*, vol. 25, no. 15, p. 18462, Jul. 2017.

[52] A. Michaels and E. Yablonovitch, “Inverse design of near unity efficiency perfectly vertical grating couplers,” *Opt. Express*, vol. 26, no. 4, p. 4766, Feb. 2018.

[53] J. Notaros *et al.*, “Ultra-Efficient CMOS Fiber-to-Chip Grating Couplers,” pp. 2–4.

[54] D. Taillaert *et al.*, “Grating couplers for coupling between optical fibers and nanophotonic waveguides,” *Japanese J. Appl. Physics, Part 1 Regul. Pap. Short Notes Rev. Pap.*, vol. 45, no. 8 A, pp. 6071–6077, Aug. 2006.

[55] D. Taillaert, H. Chong, P. I. Borel, L. H. Frandsen, R. M. De La Rue, and R. Baets, “A compact two-dimensional grating coupler used as a polarization splitter,” *IEEE Photonics Technol. Lett.*, vol. 15, no. 9, pp. 1249–1251, Sep. 2003.

[56] Y. Ding, C. Peucheret, H. Ou, and K. Yvind, “Fully etched apodized grating coupler on the SOI platform with −058 dB coupling efficiency,” *Opt. Lett.*, vol. 39, no. 18, p. 5348, Sep. 2014.

[57] H.-L. Tseng, E. Chen, H. Rong, and N. Na, “High-performance silicon-on-insulator grating coupler with completely vertical emission,” *Opt. Express*, vol. 23, no. 19, p. 24433, Sep. 2015.

[58] F. Van Laere *et al.*, “Compact and highly efficient grating couplers between optical fiber and nanophotonic waveguides,” in *Journal of Lightwave Technology*, 2007, vol. 25, no. 1, pp. 151–156.

[59] Y. Ding, C. Peucheret, H. Ou, and K. Yvind, “Fully etched apodized grating coupler on the SOI platform with −058 dB coupling efficiency,” *Opt. Lett.*, vol. 39, no. 18, p. 5348, 2014.

[60] T. K. Saha and W. Zhou, “High efficiency diffractive grating coupler based on transferred silicon nanomembrane overlay on photonic waveguide,” *J. Phys. D. Appl. Phys.*, vol. 42, no. 8, 2009.

[61] Y. Tang, Z. Wang, L. Wosinski, U. Westergren, and S. He, “Highly efficient nonuniform grating coupler for silicon-on-insulator nanophotonic circuits,” *Opt. Lett.*, vol. 35, no. 8, p. 1290, Apr. 2010.

[62] C. Alonso-Ramos, P. Cheben, A. Ortega-Moñux, J. H. Schmid, D.-X. Xu, and I. Molina-Fernández, “Fiber-chip grating coupler based on interleaved trenches with directionality exceeding 95%,” *Opt. Lett.*, vol. 39, no. 18, p. 5351, Sep. 2014.

[63] D. Benedikovic *et al.*, “L-shaped fiber-chip grating couplers with high directionality and low reflectivity fabricated with deep-UV lithography,” *Opt. Lett.*, vol. 42, no. 17, p. 3439, Sep. 2017.

[64] B. Wang, J. Jiang, and G. P. Nordin, “Embedded slanted grating for vertical coupling between fibers and silicon-on-insulator planar waveguides,” *IEEE Photonics Technol. Lett.*, vol. 17, no. 9, pp. 1884–1886, Sep. 2005.

[65] J. Schrauwen, F. Van Laere, D. Van Thourhout, and R. Baets, “Focused-ion-beam fabrication of slanted grating couplers in silicon-on-insulator waveguides,” *IEEE Photonics Technol. Lett.*, vol. 19, no. 11, pp. 816–818, Jun. 2007.

[66] S. D. Campbell, D. Sell, R. P. Jenkins, E. B. Whiting, J. A. Fan, and D. H. Werner, “Review of numerical optimization techniques for meta-device design [Invited],” *Opt. Mater. Express*, vol. 9, no. 4, p. 1842, Apr. 2019.

[67] C. Scarcella *et al.*, “Pluggable Single-Mode Fiber-Array-to-PIC Coupling Using Micro-Lenses,” *IEEE Photonics Technol. Lett.*, vol. 29, no. 22, pp. 1943–1946, Nov. 2017.

[68] H. Zuo *et al.*, “High-Performance Single-Mode Polymer Waveguide Devices for Chip-Scale Optical Interconnects,” in *2019 8th Annual IEEE Photonics Society Optical Interconnects Conference, OI 2019*, 2019.

[69] R. Dangel *et al.*, “Polymer waveguides for electro-optical integration in data centers and high-performance computers,” *Opt. Express*, vol. 23, no. 4, p. 4736, 2015.

[70] T. Mikawa *et al.*, “Implementation of active interposer for high-speed and low-cost chip level optical interconnects,” *IEEE J. Sel. Top. Quantum Electron.*, vol. 9, no. 2, pp. 452–459, 2003.

[71] L. Li *et al.*, “A fully-integrated flexible photonic platform for chip-to-chip optical interconnects,” *J. Light. Technol.*, vol. 31, no. 24, pp. 4080–4086, 2013.

[72] K. Nieweglowski, L. Lorenz, S. Lüngen, T. Tiedje, K. J. Wolter, and K. Bock, “Optical coupling with flexible polymer waveguides for chip-to-chip interconnects in electronic systems,” *Microelectron. Reliab.*, vol. 84, pp. 121–126, May 2018.

[73] T. Barwicz *et al.*, “A Novel Approach to Photonic Packaging Leveraging Existing High-Throughput Microelectronic Facilities,” *IEEE J. Sel. Top. Quantum Electron.*, vol. 22, no. 6, pp. 455–466, Nov. 2016.

[74] J. Hu, L. Li, H. Lin, P. Zhang, W. Zhou, and Z. Ma, “Flexible integrated photonics: where materials, mechanics and optics meet [Invited],” *Opt. Mater. Express*, vol. 3, no. 9, p. 1313, 2013.

[75] S. Hiramatsu and T. Mikawa, “Optical design of active interposer for high-speed chip level optical interconnects,” *J. Light. Technol.*, vol. 24, no. 2, pp. 927–933, Feb. 2006.

[76] I. K. Cho, W. J. Lee, B. S. Rho, and M. Y. Jeong, “Polymer waveguide with integrated reflector mirrors for an inter-chip link system,” *Opt. Commun.*, vol. 281, no. 19, pp. 4906–4909, Oct. 2008.

[77] O. O. Ogunsola *et al.*, “Chip-level waveguide-mirror-pillar optical interconnect structure,” *IEEE Photonics Technol. Lett.*, vol. 18, no. 15, pp. 1672–1674, Aug. 2006.

[78] X. Lin, A. Hosseini, X. Dou, H. Subbaraman, and R. T. Chen, "Low-cost board-to-board optical interconnects using molded polymer waveguide with 45 degree mirrors and inkjet-printed micro-lenses as proximity vertical coupler," *Opt. Express*, vol. 21, no. 1, p. 60, Jan. 2013.

[79] S. P. Han, J. T. Kim, S. W. Jung, S. H. Ahn, C. G. Choi, and M. Y. Jeong, "A Reflective Curved Mirror with Low Coupling Loss for Optical Interconnection," *IEEE Photonics Technol. Lett.*, vol. 16, no. 1, pp. 185–187, Jan. 2004.

[80] B.-H. (Tiger) Rhee, B. S. Rho, H. S. Cho, H.-H. Park, S. Kang, and S.-W. Ha, "PCB-Compatible Optical Interconnection Using 45°-Ended Connection Rods and Via-Holed Waveguides," *J. Light. Technol. Vol. 22, Issue 9, pp. 2128-*, vol. 22, no. 9, p. 2128, Sep. 2004.

[81] T. Gu, R. Nair, and M. W. Haney, "Prismatic coupling structure for intrachip global communication," *IEEE J. Quantum Electron.*, vol. 45, no. 4, pp. 388–395, 2009.

[82] T. Gu, R. Nair, and M. W. Haney, "Chip-level multiple quantum well modulator-based optical interconnects," *J. Light. Technol.*, vol. 31, no. 24, pp. 4166–4174, 2013.

[83] C. Choi *et al.*, "Flexible Optical Waveguide Film Fabrications and Optoelectronic Devices Integration for Fully Embedded Board-Level Optical Interconnects," *J. Light. Technol. Vol. 22, Issue 9, pp. 2168-*, vol. 22, no. 9, p. 2168, Sep. 2004.

[84] S. Yu *et al.*, "Seamless Hybrid-integrated Interconnect NEtwork (SHINE)," p. M4D.5, 2019.

[85] Q. Geng, D. Wang, P. Chen, and S. C. Chen, "Ultrafast multi-focus 3-D nano-fabrication based on two-photon polymerization," *Nat. Commun.*, vol. 10, no. 1, Dec. 2019.

[86] S. K. Saha, D. Wang, V. H. Nguyen, Y. Chang, J. S. Oakdale, and S.-C. Chen, "Scalable submicrometer additive manufacturing," *Science (80-.).*, vol. 366, no. 6461, pp. 105–109, Oct. 2019.

[87] R. A. Borisov *et al.*, "Fabrication of three-dimensional periodic microstructures by means of two-photon polymerization," *Appl. Phys. B Lasers Opt.*, vol. 67, no. 6, pp. 765–767, 1998.

[88] J. Serbin *et al.*, "Femtosecond laser-induced two-photon polymerization of inorganic–organic hybrid materials for applications in photonics," *Opt. Lett.*, vol. 28, no. 5, p. 301, Mar. 2003.

[89] J. Serbin, A. Ovsianikov, and B. Chichkov, "Fabrication of woodpile structures by two-photon polymerization and investigation of their optical properties," *Opt. Express*, vol. 12, no. 21, p. 5221, Oct. 2004.

[90] Y. Liu *et al.*, "Structural color three-dimensional printing by shrinking photonic crystals," *Nat. Commun.*, vol. 10, no. 1, Dec. 2019.

[91] N. Lindenmann *et al.*, "Photonic wire bonding: a novel concept for chip-scale interconnects," *Opt. Express*, vol. 20, no. 16, p. 17667, 2012.

[92] M. R. Billah *et al.*, "Hybrid integration of silicon photonics circuits and InP lasers by photonic wire bonding," *Optica*, vol. 5, no. 7, p. 876, Jul. 2018.

[93] A. Hofmann *et al.*, "Connecting Silicon Photonic Circuits to Multicore Fibers by Photonic Wire Bonding," *J. Light. Technol. Vol. 33, Issue 4, pp. 755-760*, vol. 33, no. 4, pp. 755–760, Feb. 2015.

[94] T. Gissibl, S. Thiele, A. Herkommer, and H. Giessen, "Two-photon direct laser writing of ultracompact multi-lens objectives," *Nat. Photonics*, vol. 10, no. 8, pp. 554–560, 2016.

[95] A. Toulouse, S. Thiele, H. Giessen, and A. M. Herkommer, "Alignment-free integration of apertures and nontransparent hulls into 3D-printed micro-optics," *Opt. Lett.*, vol. 43, no. 21, p. 5283, Nov. 2018.

[96] S. Thiele, A. Herkommer, H. Giessen, and T. Gissibl, "Sub-micrometre accurate free-form optics by three-dimensional printing on single-mode fibre," *Nat. Commun.*, vol. 7, pp. 1–9, 2016.

[97] P.-I. Dietrich *et al.*, "In situ 3D nanoprinting of free-form coupling elements for hybrid photonic integration," *Nat. Photonics*, vol. 12, no. April, 2018.

[98] O. A. Jimenez Gordillo, S. Chaitanya, Y.-C. Chang, U. D. Dave, A. Mohanty, and M. Lipson, "Plug-and-play fiber to waveguide connector," *Opt. Express*, vol. 27, no. 15, p. 20305, Jul. 2019.

[99] H. Zuo, S. Yu, T. Gu, and J. Hu, "Low loss, flexible single-mode polymer photonics," *Opt. Express*, vol. 27, no. 8, p. 11152, 2019.